



An approach based on tool mode control for surface roughness reduction in high-frequency vibration cutting

V. Ostasevicius^a, R. Gaidys^b, J. Rimkeviciene^a, R. Dauksevicius^{a,*}

^a Institute for Hi-Tech Development, Kaunas University of Technology, Studentu 65, 51369 Kaunas, Lithuania

^b Faculty of Informatics, Kaunas University of Technology, Studentu 50, 51368 Kaunas, Lithuania

ARTICLE INFO

Article history:

Received 22 January 2010

Received in revised form

25 May 2010

Accepted 28 May 2010

Handling Editor: D.J. Wagg

ABSTRACT

The presented research work, aimed at deeper understanding of vibrational process during high-frequency vibration cutting, is accomplished by treating cutting tool as an elastic structure which is characterized by several modes of natural vibrations. An approach for surface quality improvement is proposed in this paper by taking into account that quality of machined surface is related to the intensity of tool–tip (cutting edge) vibrations. It is based on the excitation of a particular higher vibration mode of a turning tool, which leads to the reduction of deleterious vibrations in the machine–tool–workpiece system through intensification of internal energy dissipation in the tool material. The combined application of numerical analysis with accurate finite element model as well as different experimental methods during investigation of the vibration turning process allowed to determine that the most favorable is the second flexural vibration mode of the tool in the direction of vertical cutting force component. This mode is excited by means of piezoelectric transducer vibrating in axial tool direction at the corresponding natural frequency, thereby enabling minimization of surface roughness and tool wear.

© 2010 Elsevier Ltd. All rights reserved.

1. Introduction

Field of metal machining is closely linked to branches of production and industry such as mechanical engineering or fabrication of mechanical components in various fields of technology. Material treatment using cutting is still one of the commonly used technological processes for manufacturing of high-precision and complex parts.

Possibility to control vibrational processes in different technological equipment is one of the approaches for enhancing efficiency. This also applies to vibrations of a cutting tool during machining operation when amplitude of induced vibrations directly influences the quality of workpiece surface. For many years the usual practice for improving surface quality was based on structural stiffening of machine tools, fixing devices and cutting tool by means of increasing cross-sections of structural elements. However, in some cases the latter approach does not provide the required final outcome. Constant pursuit for more effective cutting methods revealed that machining quality can be improved if the tool is assisted with the so-called ultrasonic frequency vibrations, which results in the reduction of cutting forces and surface roughness of a workpiece. This cutting method was termed vibration cutting [1]. Its major benefit is that a significant increase in quality of machined part can be achieved in comparison to the conventional process. As a consequence, this may lead to elimination of surface finish processes such as grinding and polishing as well as other additional machining operations.

* Corresponding author. Tel.: +37068267170; fax: +37037353637.

E-mail address: rolanas.dauksevicius@ktu.lt (R. Dauksevicius).

This aspect becomes truly significant when considering that on a global scale about US\$100 billion is spent every year on finishing of metal parts including turning, milling, boring and other cutting processes. Furthermore, it is estimated that waste constitutes about 10% of all the material produced by machining industry [2]. Another important advantage of vibration cutting is associated with reduced tool wear and possibility to treat brittle materials. In its essence vibration cutting is contrary to the conventional one: instead of aiming to diminish negative influence of vibrations by structural stiffening, vibration cutting attempts to use them to advantage. However a deeper understanding is still missing in the selection of the best working regimes of this process therefore a comprehensive investigation is required.

Vibration-assisted cutting is one of the hybrid process examples, when the cutting zone is affected by several energy forms. One of its first applications was in the field of drilling of brittle materials [3]. During this process the tool is excited with vibrations of 20–40 kHz frequency and amplitude of several micrometers. As a result, cutting forces, friction and temperature decrease in the cutting zone, tool life increases, generation of microcracks on the cutting edge and machined surface is impeded as opposed to the case of conventional cutting and grinding. Due to decrease of friction the major part of cutting energy goes to chip formation. This method opens new possibilities for treatment of glass, ceramics and hard metals [4].

There are distinguished resonance and non-resonance types of excitors of mechanical vibrations [5]. A device for excitation of elliptic motion of cutting tool vibrations is described in [6], where the tool vibrates in cutting force and feed directions. Another type of device is presented in [7], where elliptic motion is generated due to the eccentricity of indexable insert. The control of elliptic motion of this exciter is possible by attaching complementary mass. Two piezoactuators could be involved for quasi-elliptic excitation of tool vibrations [8]. It ensures the excitation of vibrations of 1 kHz with amplitude of 5 μm . The possibility to excite higher torsional mode of a turning tool is reported in Ref. [9].

According to Kim and Choi [10] effective vibration cutting occurs when the velocity of vibrations exceeds the cutting speed by 10 times. Babitsky et al. thoroughly analyzed various aspects of vibration cutting process applying both numerical and experimental methods [11–18]. Their research indicates that high-frequency vibrations transform elasto-plastic process into viscous plastic, thereby diminishing dry friction during cutting [11]. They have used vibration cutting in order to improve cutting speed and increase productivity [12], when piezoactuator at the frequency of 17 kHz excited tool vibrations of 20 μm in the feed direction, yielding cutting efficiency which corresponds to that of a high-speed process. Babitsky et al. also proposed a method for improvement of quality of machined surface, which is related to application of piezoactuator autoresonant control [13,16]. The resonance mode, maintaining the same amplitudes of tool vibrations is considered to be the best for vibration cutting [14]. Xu and Han achieved marked increase in roundness and surface quality of a workpiece by combining vibration cutting with active error compensation, which were implemented by means of two separate piezodrives [19]. Diamond tools are usually used for high-precision treatment and vibration cutting prevents the diamond insert from breaking [6]. In this case, as tool moves according to elliptic trajectory in the direction of vertical and radial components of cutting forces, it has speed component in the direction of chip formation in every cycle, just after its penetration into the machined material. The friction between tool rake face and chip effectively decreases due to alteration of friction direction, which facilitates the separation of chip better than use of cutting fluids [20]. Moriwaki and Shamoto who employed elliptic vibration cutting [21], demonstrated that cutting of brittle materials, such as glass [22] and tungsten carbides [23] could be realized by vibration cutting. During elliptic cutting the tool retreats from the workpiece, and the vertical as well as radial cutting force components are reduced. Theoretical investigation of elliptic vibration turning [24] indicates that the contact temperature effectively decreases [25]. The friction between the tool and machined surface could be diminished due to formation of oxide film layer on the rake face, which leads to the formation of thinner chips. Xiao et al. [26] point out that during vibration cutting the tool vibrations are damped, while during conventional cutting the vibrations are generated. It means that vibration cutting is more stable with respect to conventional one. Experimental and simulation results presented in [27] demonstrate that vibration cutting helps to control tool vibrations.

Wang et al. elaborate on the idea that process damping is a key factor affecting surface roughness [28]. It is demonstrated that significant contribution of the relative tool–tip vibration is associated with vibrations in the cutting force direction. A physical model is proposed to capture the dominant factor based on the process damping effect. The model with process damping factor can be utilized to establish a relationship between tool–tip vibrations and surface roughness.

Altintas and Budak [29] consider milling cutters having 2 orthogonal degrees of freedom. The cutter is assumed to have N number of teeth. The cutting forces excite the structure in the feed and normal directions, causing dynamic displacements, which are carried to rotating tooth number. The resulting chip thickness consists of static part, which is due to rigid body motion of the cutter, and the dynamic component caused by the vibrations of the tool. The methodology for the calculation of the stability lobes is related to the systems eigenvalue problem as well as calculations of critical depth and spindle speed. The stability lobes are predicted analytically and it is shown that machine tool exhibits chatter vibrations at the frequency which coincides with the second bending mode of the spindle. For the elimination of the chatter it is recommended to increase the spindle speed.

Seguy et al. in [30] examine the relationship between chatter instability and surface roughness evolution for thin wall milling. An explicit numerical model is developed for analysis of modal interactions. The model takes into account the coupling mode, the modal shape, the fact that tool may leave the ploughing effect. The paper presents surface roughness and chatter frequency measurements. Furthermore, Seguy et al. [31] deal with the effect of spindle speed variation in high-speed milling for spindle speeds corresponding to first flip (period doubling) and to the first lobes. It is demonstrated that

period doubling chatter can effectively be suppressed by spindle speed variation, although, the technique is not effective for the quasiperiodic chatter above the lobe.

The objective of the paper by Ganguli et al. [32] is to demonstrate the effect of active damping on regenerative chatter instability for turning operation. It is shown that different spindle speeds cause changes in the system damping, resulting in different levels of stability limits at different spindle speeds. It is established that low and high stability regions of the stability lobe diagram are caused by different relative positions of the poles and zeros of the system. Active damping is proposed as a strategy to enhance the stability limits of the system [32].

Initial studies, carried out by the authors of this paper in the field of vibration milling and turning [33–37], suggested new ideas for improving performance of vibration cutting processes and encouraged to perform a more thorough investigation of associated dynamic phenomena.

The main idea of the reported research work is based on treating vibration cutting tool as a flexible structure which is characterized by several modes of natural vibrations. In such machining processes as turning, milling and drilling the structural configuration of the tool resembles a cantilever beam. As it is known, the first vibration mode of a cantilever is characterized by maximum amplitudes of free end vibrations. This suggests that excitation of higher vibration modes could be beneficial for reduction of unwanted vibrations generated during machining, thereby resulting in a better quality of the workpiece. As the amplitude of higher modes becomes more intensive, energy dissipation inside tool material increases since it is considered that energy dissipated by the structure vibrating in a higher mode exceeds energy dissipated by the structure vibrating in its fundamental mode as many times as is the ratio of natural frequencies of the modes [38].

The manuscript consists of two main parts: numerical and experimental. It is organized as follows. In Chapter 2, finite element model of a vibration turning tool with piezoelectric transducer is presented. Constitutive relations used for modeling of piezoelectric behavior are provided including equation of motion of the piezoelectric transducer represented in a matrix form. The chapter is finalized with verification of the correctness of the developed model. Chapter 3 is dedicated to description of qualitative and quantitative results received during experimental investigation of vibration turning process by using vibration measurement techniques based on laser Doppler vibrometry (LDV) and holographic interferometry as well as applying surface characterization methods based on roughness measurements and imaging with scanning electron microscope. Particular emphasis is given to presentation of findings related to improvement of surface quality as well as explanation of dynamic effects, which were responsible for surface roughness reduction that was observed at specific excitation frequency of the vibration turning tool. The paper is finalized with concluding remarks.

2. Dynamic modeling and analysis of vibration turning tool

Control of vibration modes by means of experimental methods is a complex and labor-intensive task. Therefore, it is expedient to apply computational models for analysis of ultrasonic transducers. Finite element method is the predominant approach for simulation of associated dynamic processes. Piezoelectric transducers, employed in mechanical machining, usually possess higher efficiency in comparison to magnetostrictive transducers owing to lower energy losses and higher qualitative characteristics of the former. Common piezoelectric materials are used in form of stacks, functioning as actuators in vibration cutting. Positive results of vibration cutting are achieved in turning, drilling as well as milling. However, turning is the most extensively applied process worldwide therefore it is necessary to thoroughly examine the possibility to control vibration turning operation.

2.1. Finite element modeling of vibration turning tool

Piezoceramic rings were used for excitation of high-frequency vibrations in the designed and fabricated experimental prototype of the vibration turning tool [39]. Finite element (FE) software ANSYS was applied for the development of a detailed 3-D numerical model of the turning tool incorporating piezoelectric transducer (Fig. 1). The goal of the FE modeling was to reproduce the actual prototype of the vibration turning tool as accurately as possible. The model is composed of the following main parts: 1—tool insert, 2—concentrator of mechanical vibrations (horn), 3—areas of tool fixing in a lathe, 4—piezoelectric transducer (piezoceramic rings) and 5—backing.

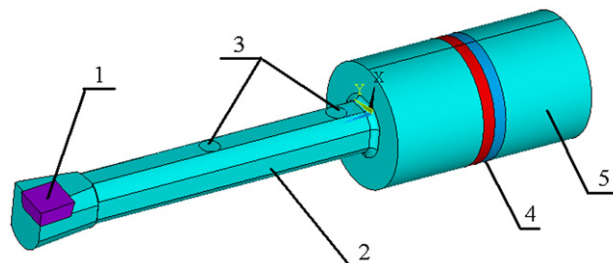


Fig. 1. Finite element model of vibration turning tool: 1—tool insert, 2—concentrator of mechanical vibrations (horn), 3—areas of tool fixing in a lathe, 4—piezoelectric transducer (piezoceramic rings) and 5—backing.

representing places where the tool is fixed in a lathe holder, 4—piezoelectric transducer (piezoceramic rings) and 5—backing (back cylinder). Values of material properties that were used for FE modeling are listed in Table 1.

When high-frequency electric impulses from generator through power amplifier are supplied to input of the piezoelectric transducer 4 it starts vibrating due to the inverse piezoeffect. These vibrations induce longitudinal waves in concentrator 2, which intensifies tool–tip vibration amplitude.

10-Node tetrahedral finite element SOLID98 with up to six degrees of freedom (dof) at each node was used for meshing of the model, which consisted of about 80,000 finite elements and 650,000 dof in total. The element has a quadratic displacement behavior and is well suited to model irregular meshes as well as to simulate mechanical structure under piezoelectric control since it is characterized by large deflection and stress stiffening capabilities. Spring elements COMBIN14 were applied for modeling of contact interaction in vibration turning tool with the purpose to achieve adequate representation of the actual character of tool fixation in the holder (Fig. 2). These elastic elements with stiffness k_i were placed at each node of fixing areas 3 (Fig. 1) and connected to immovable support. In general, COMBIN14 elements have either longitudinal or torsional capability in 1-D, 2-D or 3-D applications. In addition, the longitudinal spring–damper option is also available, which provides a massless uniaxial tension–compression element with up to three dof at each node: translations in the nodal x , y and z directions. No bending or torsion is considered in the latter case.

2.2. Formulation of dynamics of piezoelectric transducer

Modeling of piezoelectric behavior is based on the following linearized constitutive relations, which are the most widely recognized description. In the case of linear piezoelectricity the dependencies of elasticity are connected into electrostatic charge dependencies when the piezoelectric constants are averaged [40]:

$$\begin{Bmatrix} \{T\} \\ \{D\} \end{Bmatrix} = \begin{bmatrix} [c^E] & [e] \\ [e]^T & -[\epsilon^S] \end{bmatrix} \begin{Bmatrix} \{S\} \\ -\{E\} \end{Bmatrix} \tag{1}$$

where $\{T\}$ —stress vector, $\{D\}$ —electric flux density vector, $\{S\}$ —strain vector, $\{E\}$ —electric field intensity vector, $[c^E]$ —elastic compliance matrix when subjected to a constant electrical field, $[e]$ —matrix of piezoelectric stresses and $[\epsilon^S]$ —permittivity matrix measured at a constant strain.

$[c^E]$ may be represented in the following form:

$$[c^E] = \begin{bmatrix} c_{11} & c_{12} & c_{13} & c_{14} & c_{15} & c_{16} \\ & c_{22} & c_{23} & c_{24} & c_{25} & c_{26} \\ & & c_{33} & c_{34} & c_{35} & c_{36} \\ \text{Symmetry} & & & c_{44} & c_{45} & c_{46} \\ & & & & c_{55} & c_{56} \\ & & & & & c_{66} \end{bmatrix} \tag{2}$$

Table 1
Parameters used for finite element modeling of the vibration turning tool.

Component of the vibration turning tool	Material	Density ρ (kg/m ³)	Poisson's ratio ν	Young's modulus E (GPa)
Concentrator, connecting bolt, backing	Steel C45	7850	0.33	210
Piezoelectric transducer (ring-shaped)	Piezoceramics PZT5	7800	0.371	66
Tool insert	Carbide (Tungaloy grade KS05F)	15,000	0.24	640

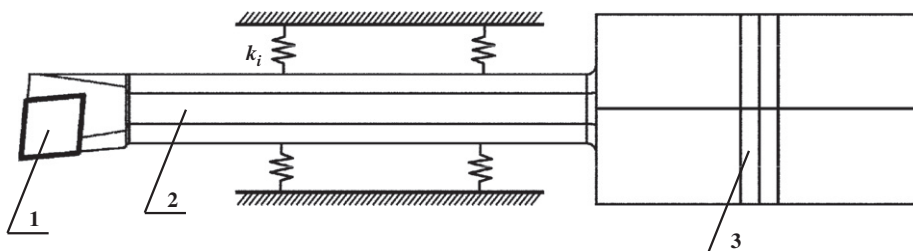


Fig. 2. Schematic representation of computation model of vibration turning tool: tool fixing areas are connected to fixed support through springs (with stiffness k_i) located at each node of the fixing area. 1—tool insert, 2—concentrator of mechanical vibrations and 3—piezoelectric transducer.

Matrix of piezoelectric stresses $[e]$ associates electric field intensity vector $\{E\}$ with stress vector $\{T\}$ and is expressed as

$$[e] = \begin{bmatrix} e_{11} & e_{12} & e_{13} \\ e_{21} & e_{22} & e_{23} \\ e_{31} & e_{32} & e_{33} \\ e_{41} & e_{42} & e_{43} \\ e_{51} & e_{52} & e_{53} \\ e_{61} & e_{62} & e_{63} \end{bmatrix} \quad (3)$$

The piezoelectric matrix $[e]$ could be used as piezoelectric strain matrix $[d]$. ANSYS automatically performs the conversion using elastic compliance matrix $[c^E]$:

$$[e] = [c^E][d] \quad (4)$$

Permittivity matrix $[\varepsilon^S]$ has the form

$$[\varepsilon^S] = \begin{bmatrix} \varepsilon_{11} & 0 & 0 \\ 0 & \varepsilon_{22} & 0 \\ 0 & 0 & \varepsilon_{33} \end{bmatrix} \quad (5)$$

Permittivity matrix measured at a constant strain acquires the following form:

$$[\varepsilon^S] = \begin{bmatrix} \varepsilon_{11} & \varepsilon_{12} & \varepsilon_{13} \\ & \varepsilon_{22} & \varepsilon_{23} \\ \text{Symmetry} & & \varepsilon_{33} \end{bmatrix} \quad (6)$$

ANSYS automatically converts permittivity matrix measured at a constant stress $[\varepsilon^T]$ into permittivity matrix measured at a constant strain:

$$[\varepsilon^S] = [\varepsilon^T] - [e]^T[d] \quad (7)$$

Equation of motion of the piezoelectric transducer in a matrix form is written as follows:

$$\begin{bmatrix} M_{uu} & 0 \\ 0 & 0 \end{bmatrix} \begin{Bmatrix} \ddot{u} \\ \dot{\phi} \end{Bmatrix} + \begin{bmatrix} K_{uu} & K_{u\phi} \\ K_{u\phi}^T & K_{\phi\phi} \end{bmatrix} \begin{Bmatrix} u \\ \phi \end{Bmatrix} = \begin{Bmatrix} F_S \\ Q_S \end{Bmatrix} \quad (8)$$

with uncoupled boundary conditions

$$\{u\} = 0 \quad (9)$$

$$\{\phi\} = \{\phi_0\} \quad (10)$$

where $\{u\}$ —mechanical displacement degrees of freedom, $\{\phi\}$ —electric potential degrees of freedom, $[M_{uu}]$ —mass matrix, $[K_{uu}]$ —mechanical stiffness matrix, $[K_{u\phi}]$ —piezoelectric coupling matrix, $[K_{\phi\phi}]$ —dielectric stiffness matrix, $[F_S]$ —mechanical surface forces—equal to zero, $[Q_S]$ —electric surface forces and $\{\phi_0\}$ —the specified electric potential.

2.3. Evaluation of model accuracy

Development of physically adequate FE model of the vibration turning tool was essential in order to be able to provide reliable clarification of experimental findings presented in the next chapter (particularly the results indicating marked improvement of surface roughness at particular excitation frequency (17.1 kHz) of vibration turning tool (see Fig. 10)). The degree of conformity between experimental and simulated resonant frequencies of the tool was adopted as a criterion defining accuracy of the numerical model. The critical step in FE modeling was to accurately reproduce the actual contact interaction in the tool fixing areas by selecting appropriate stiffness k_i values of COMBIN14 elastic elements, which were defined in the nodal x , y and z directions. To this aim the model was subjected to a series of frequency response analyses conducted by varying values of stiffness k_i . During simulations the piezoelectric transducer was harmonically excited with voltage of 100 V in a frequency range of 10–30 kHz. Fig. 3 illustrates several representative amplitude–frequency characteristics of the tool–tip obtained at different stiffness values, which were expressed in terms of magnitude of Young’s modulus E of steel grade C45 that was used for fabrication of the concentrator and backing of the tool (Table 1). It is obvious from Fig. 3 that larger stiffness values lead to higher resonant frequencies. Accuracy of the FE model was judged by comparing simulated frequency responses in Fig. 3 with the experimental ones (see Fig. 6). The objective of adjusting stiffness k_i was to attain a reasonably close agreement between simulated and measured values of resonant frequencies, particularly for the case of the most significant frequency of 17.1 kHz. Thus, stiffness values were modified until simulated resonance peaks in all three directions of the cutting force were located as close as possible to the experimental value of 17.1 kHz. Frequency response curves marked as “E/10” (solid blue line) in Fig. 3 demonstrate that the best match between simulation and experimental results is achieved when stiffness k_i is equal in magnitude to the 1/10th of Young’s modulus of steel grade C45. At this particular stiffness value simulated resonance peaks at 17.19 kHz are present in all cutting force

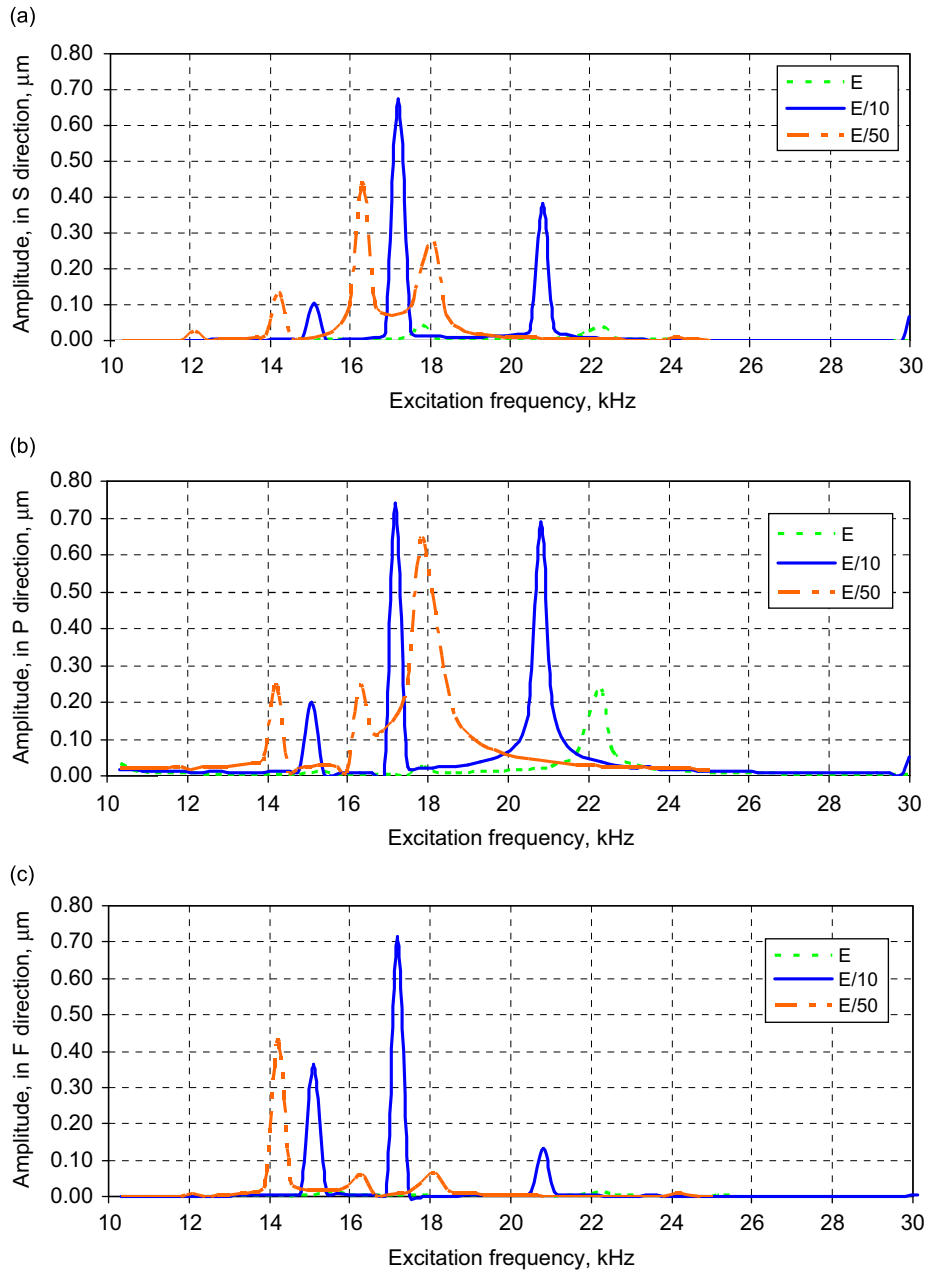


Fig. 3. Simulated frequency response characteristics of tool cutting edge obtained at different contact stiffness values, which are expressed in terms of magnitude of Young's modulus E of steel C45: (a)—direction of vertical cutting force component S , (b)—direction of radial cutting force component P and (c)—direction of axial cutting force component (feed direction) F .

directions. The accuracy of the final FE model is evaluated quantitatively by calculating relative error using numerical and experimental values of the considered resonant frequency: $\delta = (|17.1 - 17.19|/17.1) \times 100 = 0.53\%$. This value thereby confirms the ability of the developed FE model of the vibration turning tool to provide sufficiently reliable numerical results in the frequency domain.

2.4. Numerical modal analysis

Subsequently, the FE model was subjected to numerical modal analysis in order to determine the mode shapes that are excited at particular frequencies of interest. Fig. 4 presents results of the simulations. Fig. 4(a) reveals that excitation frequency of 15.11 kHz induces tool-tip vibration mode in the direction of axial cutting force component (feed direction) F (directions are illustrated in Fig. 5). This mode corresponds to the second flexural mode of a cantilever; meanwhile, in

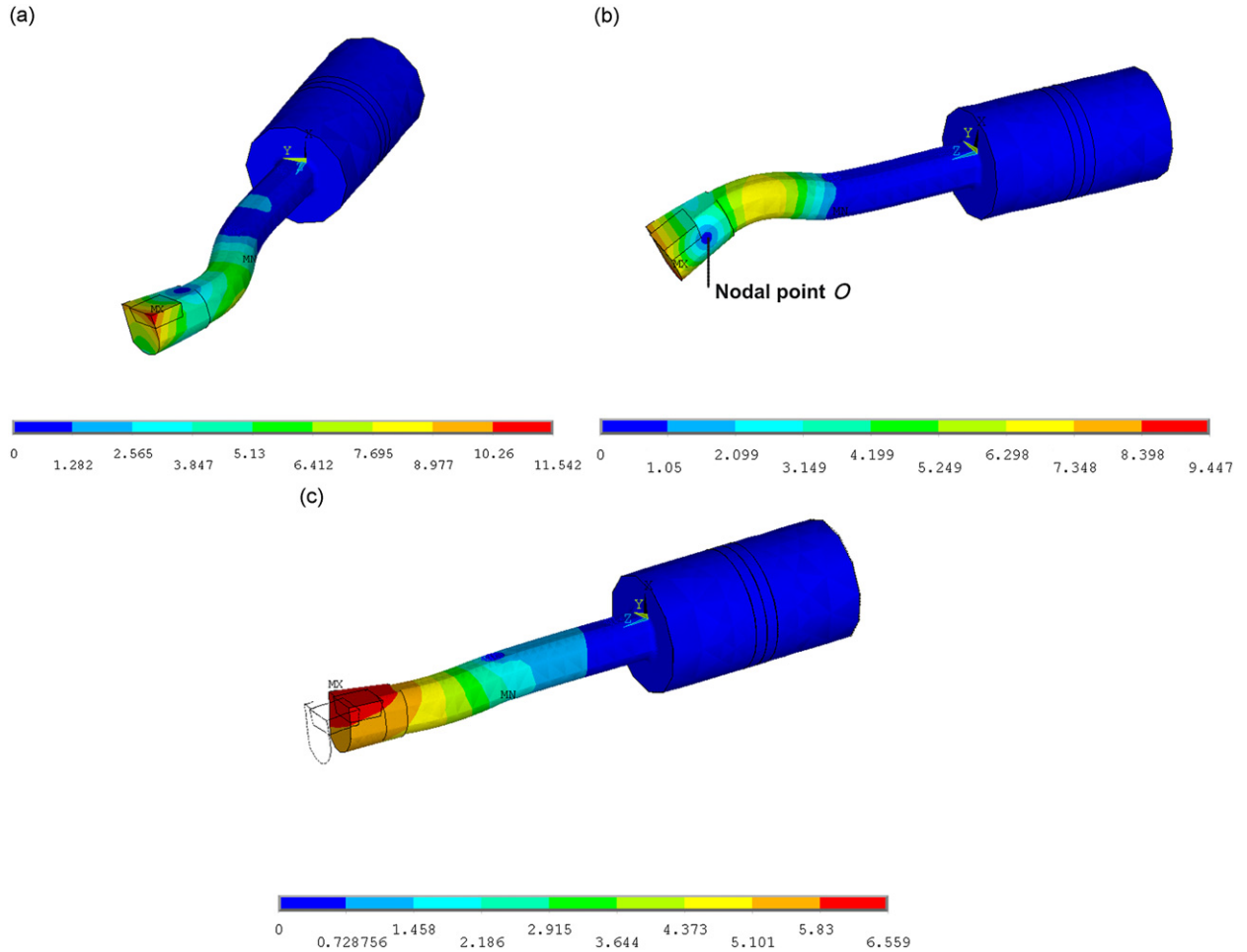


Fig. 4. Simulated natural vibration modes of the turning tool: (a)—the 2nd flexural mode in the direction of axial cutting force component (feed direction) F (15.11 kHz), (b)—the 2nd flexural mode in the direction of vertical cutting force component S (17.19 kHz) and (c)—longitudinal mode in the direction of radial cutting force component P (20.82 kHz).

Fig. 4(b) we observe that the second flexural mode in the vertical cutting force direction S manifests at the frequency of 17.19 kHz. Next dominant frequency is 20.82 kHz, which corresponds to the tool vibration mode in the direction of radial cutting force component P , which is equivalent to the first longitudinal vibration mode of a cantilever (Fig. 4(c)). The results of numerical modal analysis demonstrate that longitudinal waves generated by the piezoelectric transducer excite both longitudinal and transverse vibrations of the tool-tip, particularly at the resonant frequencies of the concentrator in feed or vertical cutting force directions. A closer look at the vibration mode in Fig. 4(b) reveals that the horn oscillates around immovable point corresponding to the nodal point O of the second flexural mode in vertical cutting force direction S . This indicates that at the resonant frequency of 17.19 kHz the tool-tip vibration amplitude is significantly reduced in comparison to the amplitude of the first flexural mode, which frequency is about 6 times lower with respect to the second mode.

3. Experimental research of vibration cutting

In general, vibration turning experiments may be performed for two cases: (a) rough turning, when the goal is to maximize volume of removed material and the cutting process is more influenced by high-frequency tool-tip vibrations in feed direction, and (b) finish turning, when surface quality is of primary importance and performance of the process is more determined by tool-tip vibrations generated in the direction of vertical and radial cutting force components. Our research work is devoted to the latter case and the aim is to characterize vibration turning process in terms of surface quality improvement. Therefore, different types of experiments were carried out, providing both qualitative and quantitative results on the subject matter.

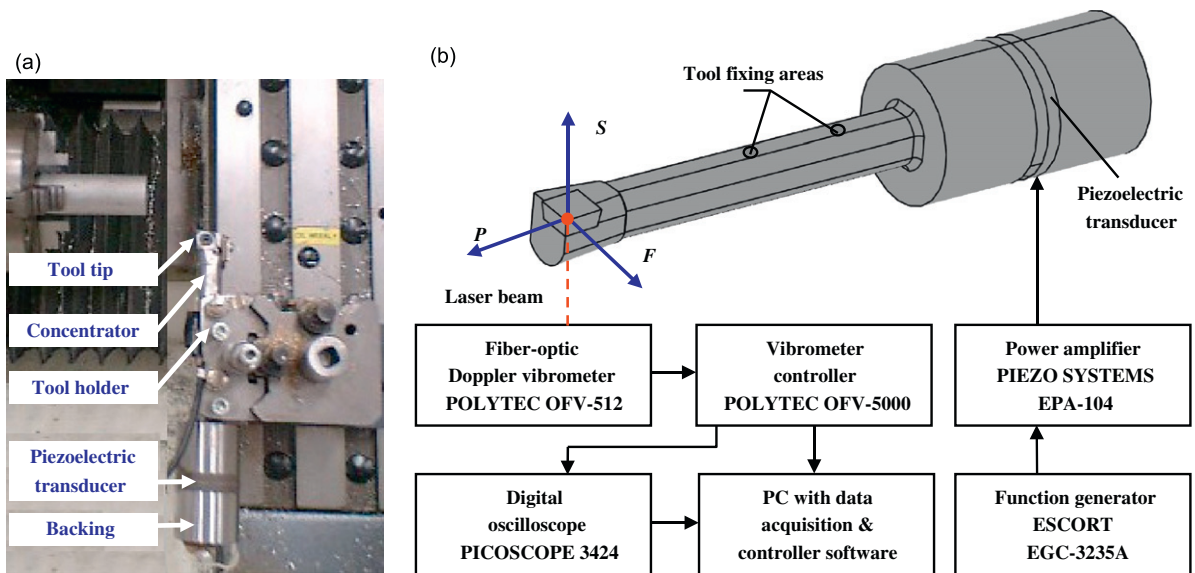


Fig. 5. (a) Vibration turning tool mounted in CNC lathe DENFORD EO4621. (b) Schematics of experimental setup for measurement of tool-tip frequency response characteristics.

3.1. Tool-tip vibration measurements by laser Doppler vibrometry

Laser Doppler vibrometry (LDV) was applied for frequency response measurements of the vibration turning tool mounted in CNC lathe DENFORD EO4621 (Fig. 5(a)). The registered amplitude–frequency characteristics of the tool-tip were used to verify the accuracy of the developed finite element model of the tool (see Chapter 2.3).

Schematic representation of the experimental setup is given in Fig. 5(b). The tool was fixed in the holder in two places. The conditions of tool fixation strongly affect results of dynamic measurements, which are particularly sensitive to variations in bolt fastening force as well as location and number of fixation places. Piezoelectric transducer was driven harmonically by using function generator ESCORT EGC-3235A. A constant excitation voltage of 100 V was maintained by power amplifier PIEZO SYSTEMS EPA-104. Polytec fiber-optic Doppler interferometer OFV-512 in conjunction with controller OFV-5000 were used to measure vibration amplitudes of the tool-tip (insert cutting edge) in three cutting force directions (Fig. 5(b)): S —direction of vertical cutting force component, P —direction of radial cutting force component and F —direction of axial cutting force component (feed direction). Measured signals were captured by digital oscilloscope PICOSCOPE-3424 and transferred to a personal computer for subsequent processing and visualization of the results. Measurements were conducted in excitation frequency range of 8–40 kHz. The resulting amplitude–frequency characteristics (Fig. 6) reveal that tool-tip vibration amplitudes are insignificant beyond this range. Presented characteristics reflect major resonant frequencies that are exhibited by the vibration turning tool as well as provide useful information about direction of vibrations. It should be noted that at resonant frequencies of 13, 17.1 and 21.3 kHz piezoelectric transducer excites tool-tip vibrations in several cutting force directions, which indicates that elliptical tool-tip motion is generated at these frequencies.

3.2. Evaluation of workpiece surface roughness and tool wear

A suitable approach for evaluation of contact interaction between a turning tool and workpiece is to employ surface roughness. Measured surface roughness values of machined workpieces confirm that vibration cutting improves surface quality for different types of materials. With the purpose of assuring surface quality of components machined using vibration turning, quality control system (Fig. 7) was developed and approved as invention by patent [41]. The system consists of (a) vibration turning tool with vibration sensor, which is rigidly attached onto the backing and connected in parallel to the autoresonant control block, (b) acoustic emission (AE) sensor, which is rigidly attached to the nonworking surface of the tool and is connected to the control block through power amplifier and frequency filter that are linked in series. Resonant excitation of the system is maintained by the autoresonant control block, which uses signals from the vibration sensor in order to provide the required excitation. During vibration turning operation the amplified and filtered signal from the AE sensor is fed into the control block, where it is analyzed in order to separate from the frequency spectrum a component that is characteristic to the turning process, which is terminated when critical value of the separated spectral component is reached. In this way the system controls tool wear-out, simultaneously allowing to assure surface quality of the workpiece. Experimental results indicate that the most informative AE signals are located within the

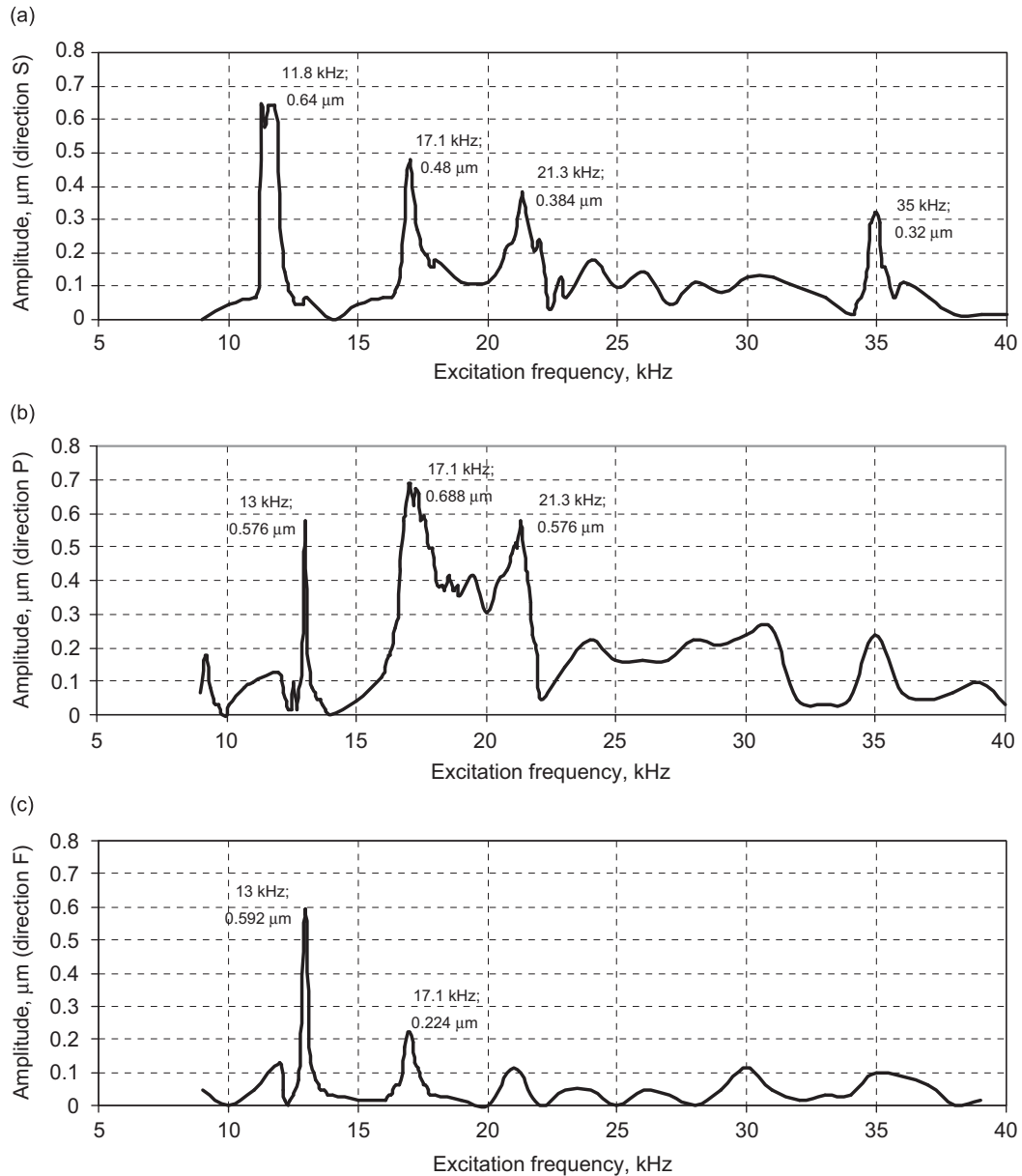


Fig. 6. Measured frequency response characteristics of tool cutting edge: (a)—direction of vertical cutting force component S , (b)—direction of radial cutting force component P and (c)—direction of axial cutting force component (feed direction) F .

range of 50–80 kHz, which provides information about dry friction. Comparison of measured AE signals (Fig. 8) reveals that in the case of vibration turning of aluminum workpieces the signals are lower with respect to the case of conventional process. This implies that friction is reduced during vibration cutting. Analogous results were also obtained for workpieces made of steel and brass.

Multiple experiments were carried out with intention to demonstrate surface roughness improvement and tool wear reduction during vibration cutting. Two workpieces were machined using identical cutting parameters: feed f —0.1 mm/rot, spindle rotation n —1800 rot/min and cutting depth a —0.25 mm. For both workpieces 12 cutting passes of ≈ 15 mm length were performed. Surface of the workpieces was qualitatively analyzed by means of scanning electron microscope (SEM) JEOL JSM-IC25S. Obtained images (Fig. 9) provide a visual indication that the surface of workpieces machined with vibration turning is smoother in comparison to the conventional process. Furthermore, it was observed that microcracks are absent in the former case. In addition, it is evident from closer inspection of SEM images that workpiece surface after traditional turning (Fig. 9(a)) resembles a “roughly ploughed field”, which refers to instability of the cutting process.

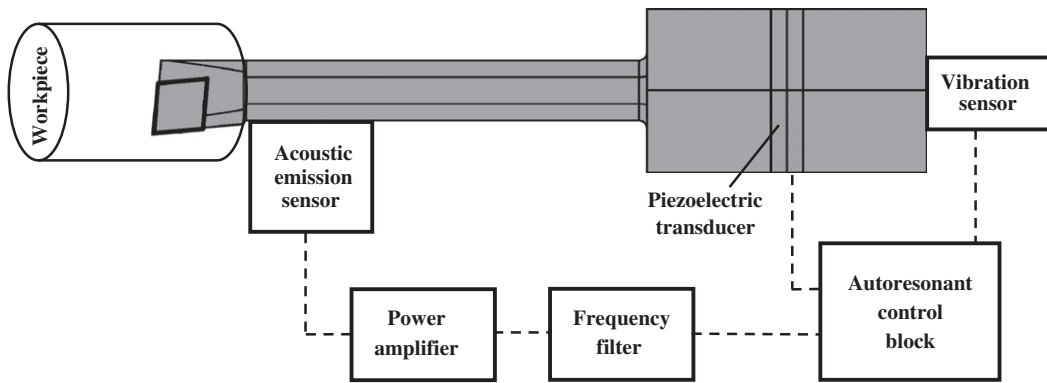


Fig. 7. Principal scheme of the developed control system for assurance of quality of a machined surface during vibration turning.

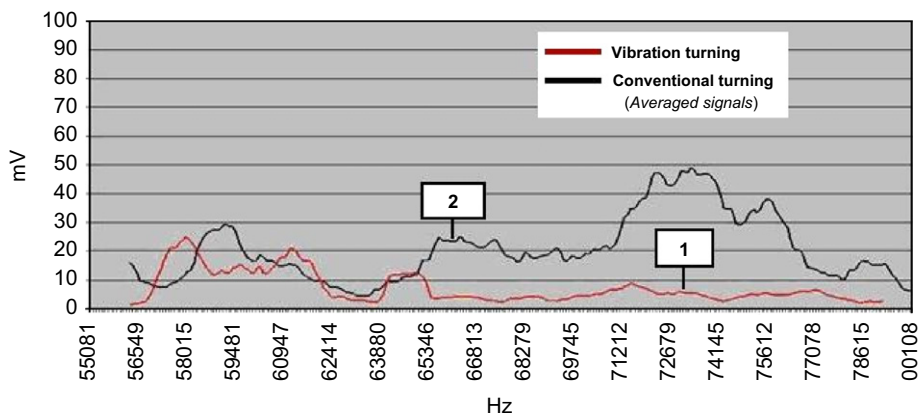


Fig. 8. Acoustic emission signals during turning process of aluminum workpiece: 1—during vibration turning and 2—during conventional turning.

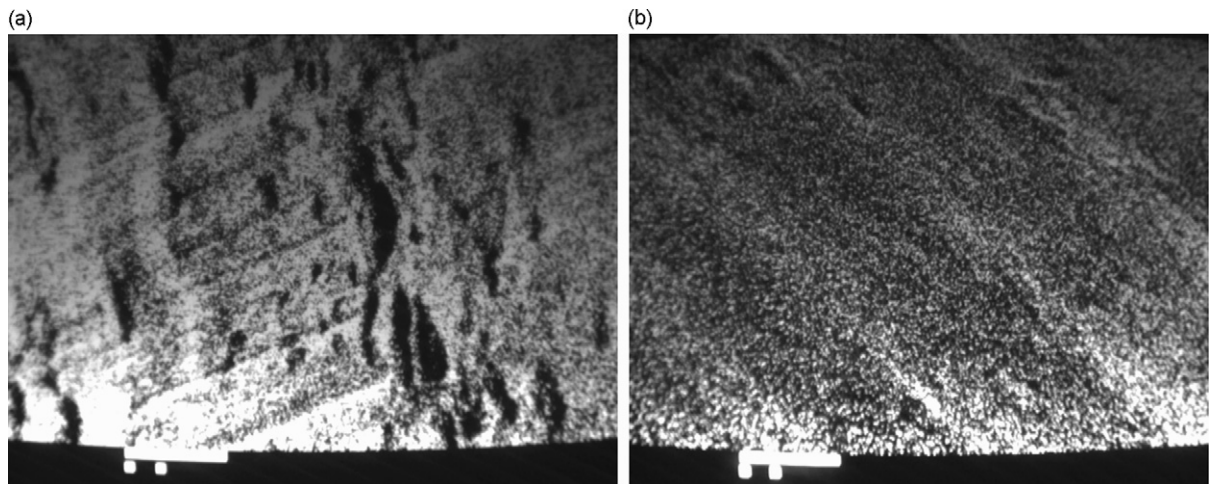


Fig. 9. SEM images of surface of machined workpiece (2000 ×, length of white bar=10 μm): (a)—after conventional turning and (b) after vibration turning.

Meanwhile, vibration turning produces a surface (Fig. 9(b)) that is similar to a “cultivated field”, which is characterized by strictly regular fine-meshed structure.

Roughness meter Mitutoyo Surftest SJ-201 was used to obtain quantitative results about surface roughness of aluminum workpieces turned with and without superimposed vibrations (feed $f=0.05$ mm/rot, spindle rotation

$n=1900$ rot/min and cutting depth $a=0.25$ mm). The value of $R_a=191 \pm 003 \mu\text{m}$, measured after conventional turning, reveals that surface roughness in the case of vibration turning at 17.1 kHz (Fig. 10)— $R_a=081 \pm 002 \mu\text{m}$ —is approximately one roughness grade number lower with respect to conventional process (according to DIN EN ISO 1302).

A series of turning experiments were performed with the purpose of determining the magnitude of tool excitation frequency for which the best surface quality is obtained. These experiments were carried out using the following parameters: feed $f=0.05$ mm/rot, spindle rotation $n=1900$ rot/min, cutting depth $a=0.25$ mm and excitation frequencies—11.8, 12.9, 13, 17.1, 21.3, 26.2 and 27.3 kHz. These values were selected since vibration measurement results in Fig. 6 indicate that these frequencies correspond to the most clearly expressed amplitude peaks. Meaningful results were received when measured roughness values were plotted as a function of tool excitation frequency (Fig. 10). The plot reveals that the lowest surface roughness of aluminum workpiece is observed at 17.1 kHz. At this frequency the piezoelectric transducer excites tool–tip vibrations which are dominant in vertical and radial components of the cutting force (see Fig. 6(a) and (b)). It is important to emphasize that according to the results of numerical modal analysis this particular frequency corresponds to the second flexural vibration mode of the tool in the vertical cutting force direction S (see Fig. 4(b)). In other words, when the tool is excited with 17.1 kHz its cutting edge executes high-frequency low-amplitude motion around nodal point O of the second flexural vibration mode in vertical direction S . These results imply that excitation of this vibration mode is advantageous in achieving the best surface quality of the workpiece. It could be reasoned that the physical mechanism that is responsible for surface roughness reduction at the 17.1 kHz is related to more intensive energy dissipation inside tool material when the tool vibrates in the second flexural mode since it is considered [38] that energy dissipated by the structure vibrating in the higher mode exceeds energy dissipated by the structure vibrating in its fundamental mode as many times as is the ratio of natural frequencies of the modes. In the considered case, the frequency of the second flexural mode is about 6 times larger than the first flexural mode. Consequently, excitation of the second flexural mode of the tool at 17.1 kHz leads to the corresponding 6-fold increase in energy dissipated inside the tool material. This, in turn, suggests that at this particular excitation frequency the cutting tool becomes a more effective damper, which considerably contributes to the suppression of deleterious vibrations generated in the system during cutting process thereby favoring chatter mitigation.

Influence of vibration cutting on tool wear was analyzed by examining cutting inserts with SEM. Obtained images (Fig. 11) provide a visual evidence that cutting edge of the new insert is neither deformed nor damaged. Tool insert that was used during vibration cutting essentially does not differ from the new one and is nearly undamaged (Fig. 11(b)), whereas image of the insert after conventional turning reveals clearly visible deterioration of the cutting edge, which is characterized by irregular and chipped contour (Fig. 11(c)). These findings confirm that vibration cutting leads to reduced tool wear in comparison to the conventional process.

3.3. Measurement of tool mode shapes by holographic interferometry

Holographic interferometry setup (Fig. 12(a)) based on HYTEC PRISM deformation and vibration measurement system was used to determine higher vibration modes of the turning tool. Deformed shapes of the tool were recorded at different harmonic excitation frequencies (Fig. 12(b)–(d)). Provided results confirm that simulated vibration mode shapes obtained by numerical modal analysis are in agreement with the experimental shapes. Fig. 12(b) indicates that at 13 kHz the tool vibrates in the second flexural mode in the direction of axial cutting force component (feed direction) F , which corresponds

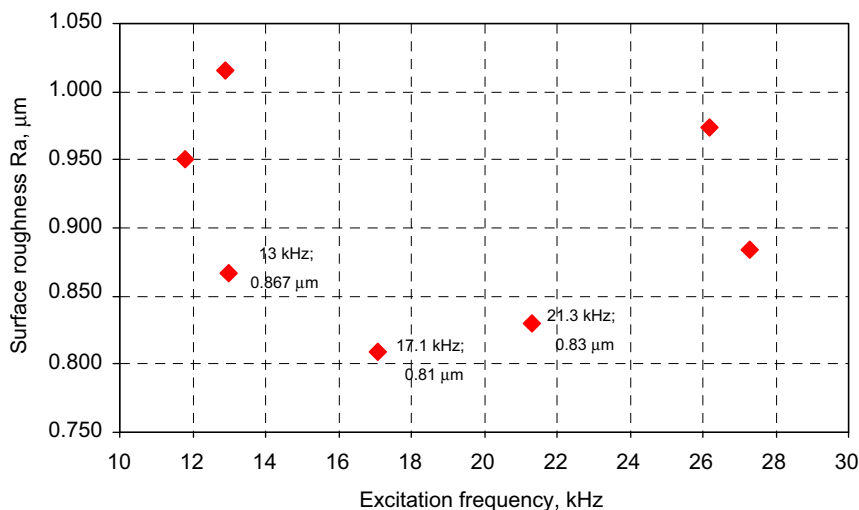


Fig. 10. Measured values of surface roughness R_a of aluminum workpiece after vibration turning by using different excitation frequencies of the cutting tool.

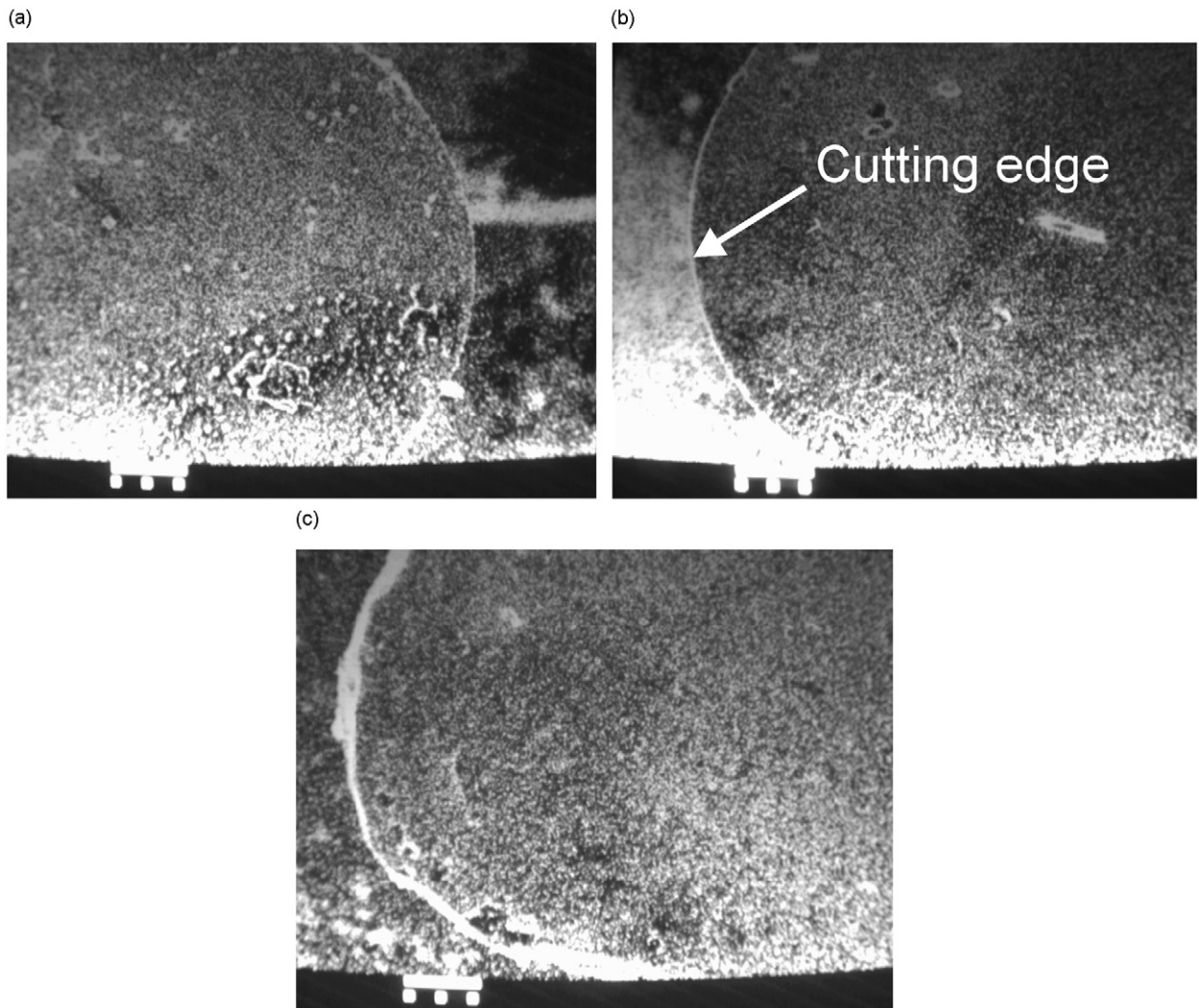


Fig. 11. SEM images of cutting edge of turning tool insert ($100\times$, length of white bar= $100\ \mu\text{m}$): (a) new tool insert, (b)—tool insert used in vibration turning and (c)—tool insert used in conventional turning.

to the simulated vibration shape at $15.11\ \text{kHz}$ in Fig. 4(a). Holographic image in Fig. 12(c) obtained at $17.1\ \text{kHz}$ reveals the second flexural mode in the direction of vertical cutting force component S , which is in good agreement with vibration shape prediction at $17.19\ \text{kHz}$ illustrated in Fig. 4(b). Finally, vibration mode shape registered at $21.3\ \text{kHz}$ and presented in Fig. 12(d) is a manifestation of longitudinal vibration mode in the direction of radial cutting force component P , which well corresponds to the simulated vibration shape at $20.82\ \text{kHz}$ in Fig. 4(c).

4. Discussion and conclusions

The research work presented in this paper was undertaken by the authors in pursuit to find a simple yet effective means for enhancing surface quality of a workpiece which is machined by using vibration turning. This work stems from and is mainly motivated by earlier theoretical and experimental findings in the field of elastic vibro-impact systems, where advantageous utilization of higher vibration modes provided significant improvements in dynamic performance of the investigated nonlinear mechanical systems.

This paper has considered an approach enabling to reduce surface roughness of the machined workpiece by means of excitation of the second flexural mode of the vibration turning tool in the direction of vertical cutting force component. Successful application of hybrid numerical-experimental analysis allowed us to receive reliable results that clearly support the validity of the proposed idea. First of all, experimental investigation of vibration cutting was conducted by using the developed vibration turning tool with the purpose to establish the value of excitation frequency which yields the highest

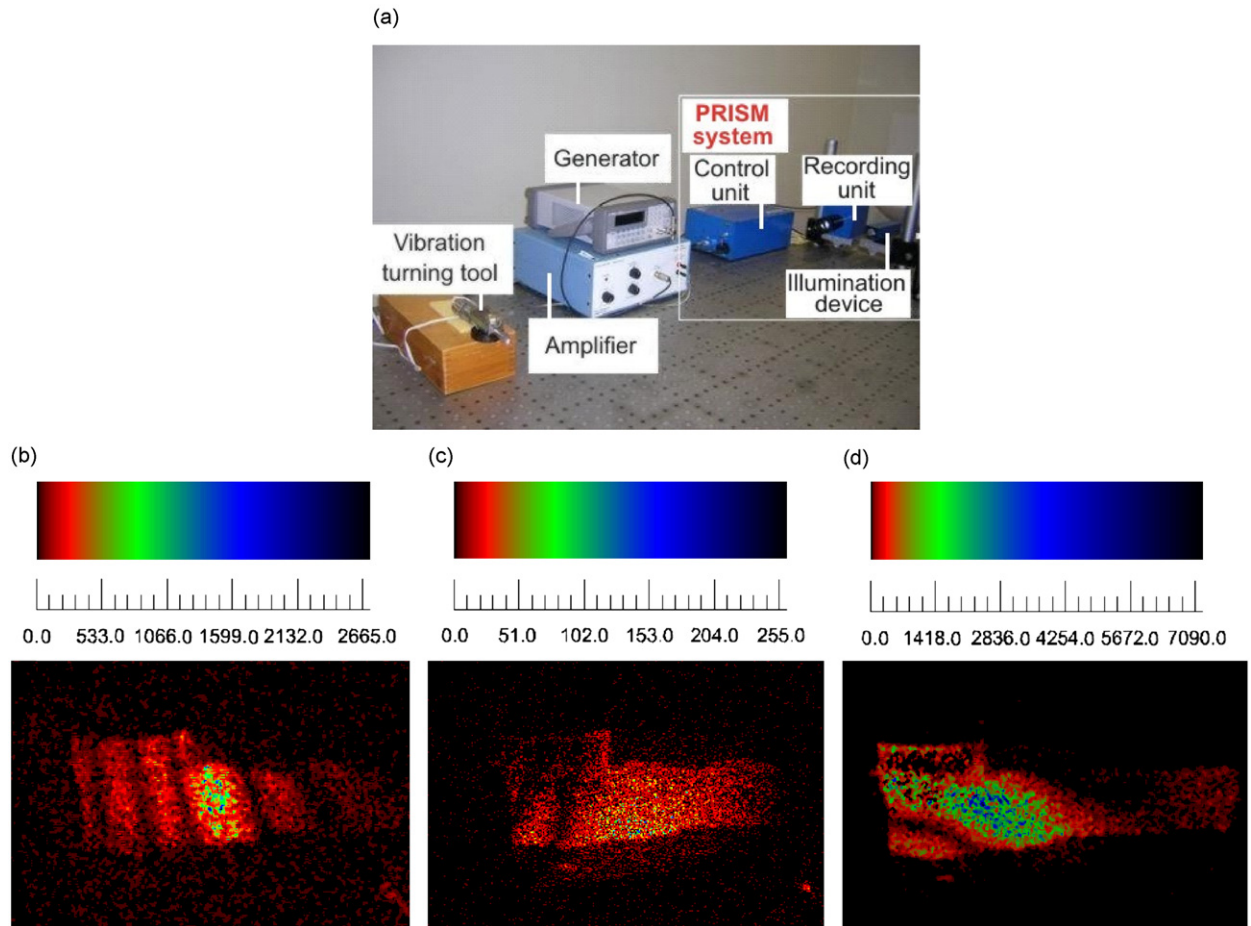


Fig. 12. (a) Experimental setup based on holographic interferometry system HYTEC PRISM for measurement of vibration modes of the vibration turning tool. (b)–(d) Holographic images of mode shapes of the vibration turning tool measured in axial cutting force component (feed direction) F : (b)—mode shape at 13 kHz, (c)—mode shape at 17.1 kHz and (d)—mode shape at 21.3 kHz.

surface quality. Measurement results revealed that the lowest surface roughness of the workpiece is achieved at 17.1 kHz. Subsequently, frequency response characteristics, registered by LDV-based experimental setup, demonstrated that at the frequency of 17.1 kHz tool–tip vibrations are excited in two predominant directions, which correspond to vertical and radial components of the cutting force. Next, a detailed 3-D finite element model of the turning tool with piezoelectric transducer was developed and experimentally verified. This enabled to perform accurate simulations aiming to identify the underlying dynamic phenomena associated with the experimental findings as well as to provide adequate interpretation of the results. Comparison of experimental and numerical results led to the conclusion that the highest surface quality of the machined workpiece is obtained when the second flexural mode of the tool concentrator is excited in the direction of vertical cutting force component. The positive effect of this higher vibration mode on surface quality is attributed to the increased energy dissipation inside tool material during excitation of the mode. As a consequence, the tool starts to function as an effective dampening element, which abates detrimental influence of unwanted vibrations generated in the machine–tool–workpiece system during turning process. In other words, we believe that reduction of surface roughness in this case is achieved through intensified chatter suppression which occurs during excitation of the considered higher vibration mode at the frequency of 17.1 kHz.

In addition, presented research work also demonstrates that it is possible to avoid application of complex asymmetrical form of the tool in order to generate particular motion of the cutting edge. Instead, it is sufficient to excite a specific vibration mode of the tool in order to achieve the required tool–tip trajectory.

In conclusion, obtained research results enabled us to propose a feasible solution for improvement of surface quality of the workpiece by virtue of advantageous application of the specific higher vibration mode of the cutting tool. This, in turn, has important practical implications for the development of efficient vibration cutting equipment since the presented approach of tool mode control is relatively simple to implement in industrial environment as it does not require sophisticated control devices.

References

- [1] J. Kumabe, in: *Vibration Cutting*, Jikkyo Publishing, Tokyo, 1979.
- [2] V.S. Sharma, M. Dogra, N.M. Suri, Advances in the turning process for productivity improvement—a review, *Proceedings of the Institution of Mechanical Engineers, Part B: Journal of Engineering Manufacture* 222 (11) (2008) 1417–1442.
- [3] O.V. Abramov, in: *High-intensity Ultrasonics, Theory and Industrial Applications*, Gordon and Breach Science Publishers, Amsterdam, 1998.
- [4] F. Klocke, O. Rubenach, Ultrasonic assisted diamond turning of steel and glass, *Proceedings of the International Seminar on Precision Engineering and Micro Technology*, Aachen, July 2000, pp. 179–190.
- [5] M.A. Cerniway, Elliptical Diamond Milling: Kinematics, Force and Tool Wear, MS Thesis, North Carolina State University, 2001.
- [6] E. Shamoto, T. Moriwaki, Study on elliptical vibration cutting, *Annals of the CIRP* 43 (1) (1994) 35–38.
- [7] E. Brinksmeir, R. Glabe, Elliptical vibration cutting of steel with diamond tools, *Proceedings of the 14th Annual ASPE Meeting*, Monterey, October 1999, pp. 163–166.
- [8] A. Jung-Hwan, L. Han-Seok, S. Seong-Min, Improvement of micro-machining accuracy by 2-dimensional vibration cutting, *Proceedings of the 14th Annual ASPE Meeting*, Monterey, October 1999, pp. 150–153.
- [9] T. Moriwaki, E. Shamoto, Ultra-precision diamond cutting of hardened steel by applying elliptical vibration cutting, *Annals of the CIRP* 48 (1999) 441–444.
- [10] J.D. Kim, I.H. Choi, Micro surface phenomenon of ductile cutting in the ultrasonic vibration cutting of optical plastics, *Journal of Materials Processing Technology* 68 (1997) 89–98.
- [11] V.K. Astashev, V.I. Babitsky, Ultrasonic cutting as a nonlinear (vibro-impact) process, *Ultrasonics* 36 (1998) 89–96.
- [12] V.I. Babitsky, A.N. Kalashnikov, A. Meadows, A.A.H.P. Wijesundara, Ultrasonically assisted turning of aviation materials, *Journal of Materials Processing Technology* 132 (2003) 157–167.
- [13] V.I. Babitsky, A.N. Kalashnikov, F.V. Molodtsov, Autoresonant control of ultrasonically assisted cutting, *Mechatronics* 14 (2004) 91–114.
- [14] V.I. Babitsky, V.K. Astashev, Nonlinear dynamics and control of ultrasonically assisted machining, *Journal of Vibration and Control* 13 (5) (2007) 441–460.
- [15] N. Ahmed, A.V. Mitrofanov, V.I. Babitsky, V.V. Silberschmidt, Analysis of forces in ultrasonically assisted turning, *Journal of Sound and Vibration* 308 (2007) 845–854.
- [16] S. Voronina, V.I. Babitsky, Autoresonant control strategies of loaded ultrasonic transducer for machining applications, *Journal of Sound and Vibration* 313 (2008) 395–417.
- [17] V.I. Babitsky, V.K. Astashev, A. Meadows, Vibration excitation and energy transfer during ultrasonically assisted drilling, *Journal of Sound and Vibration* 308 (2007) 805–814.
- [18] P.N.H. Thomas, V.I. Babitsky, Experiments and simulations on ultrasonically assisted drilling, *Journal of Sound and Vibration* 308 (2007) 815–830.
- [19] W.L. Xu, L. Han, Piezoelectric actuator based active error compensation of precision machining, *Measurement Sciences and Technology* 10 (1999) 106–111.
- [20] N. Suzuki, A. Nakamura, E. Shamoto, K. Harada, M. Matsuo, M. Osada, Ultraprecision micromachining of hardened steel by applying ultrasonic elliptical vibration cutting, *Proceedings of the International Symposium on Micromechatronics and Human Science*, October 2003, Nagoya, pp. 221–226.
- [21] T. Moriwaki, E. Shamoto, Ultrasonic elliptical vibration cutting, *CIRP Annals—Manufacturing Technology* 44 (1995) 31–34.
- [22] T. Moriwaki, E. Shamoto, Ultraprecision ductile cutting of glass by applying ultrasonic vibration, *Annals of the CIRP* 41 (1992) 141–144.
- [23] N. Suzuki, S. Masuda, E. Shamoto, Ultraprecision machining of sintered tungsten carbide by applying ultrasonic elliptical vibration cutting, *Proceedings of the Fourth International Conference of the EUSPEN*, Glasgow, May–June 2004, pp. 187–188.
- [24] C.X. Ma, E. Shamoto, T. Moriwaki, L.J. Wang, Study of machining accuracy in ultrasonic elliptical vibration cutting, *International Journal of Machine Tools and Manufacture* 44 (2004) 1305–1310.
- [25] M. Jin, M. Murakawa, Development of a practical ultrasonic vibration cutting tool system, *Journal of Materials Processing Technology* 113 (2001) 342–347.
- [26] M. Xiao, K. Sato, S. Karube, T. Soutome, The effect of tool nose radius in ultrasonic vibration cutting of hard metal, *International Journal of Machine Tools and Manufacture* 43 (2003) 1375–1382.
- [27] M. Xiao, S. Karube, T. Soutome, K. Sato, Analysis of chatter suppression in vibration cutting, *International Journal of Machine Tools and Manufacture* 42 (2002) 1677–1685.
- [28] H. Wang, S. To, C.Y. Chan, C.F. Chang, W.B. Lee, A theoretical and experimental investigation of the tool–tip vibration and its influence upon surface generation in single-point diamond turning, *International Journal of Machine Tools and Manufacture* 50 (2009) 241–252.
- [29] Y. Altintas, E. Budak, Analytical prediction of stability lobes in milling, *Annals of the CIRP* 44 (1995) 357–362.
- [30] S. Seguy, G. Dessein, L. Arnaud, Surface roughness variation of thin wall milling, related to modal interactions, *International Journal of Machine Tools and Manufacture* 48 (2008) 261–274.
- [31] S. Seguy, T. Insperger, L. Arnaud, G. Dessein, G. Peigné, On the stability of high-speed milling with spindle speed variation, *International Journal of Advanced Manufacturing Technology* doi:10.1007/s00170-009-2336-9.
- [32] A. Ganguli, A. Deraemaeker, A. Preumont, Regenerative chatter reduction by active damping control, *Journal of Sound and Vibration* 300 (2007) 847–862.
- [33] J. Grazeviciute, I. Skiedraite, V. Ostasevicius, V. Jurenas, A. Bubulis, Ultrasound application in turning process, *Proceedings of the Sixth International Conference Vibroengineering*, Kaunas, October 2006, pp. 152–154.
- [34] J. Grazeviciute, I. Skiedraite, V. Jurenas, A. Bubulis, V. Ostasevicius, Applications of high frequency vibrations for surface milling, *Mechanika* 1 (2008) 46–49.
- [35] J. Grazeviciute, R. Gaidys, V. Jurenas, V. Ostasevicius, Influence of turning tool dynamics on surface quality of work piece, *Proceedings of the 13th International Conference Mechanika*, Kaunas, April 2008, pp. 149–152.
- [36] J. Rimkeviciene, R. Gaidys, V. Jurenas, V. Ostasevicius, Research of ultrasonic assisted turning tool, *Journal of Vibroengineering* 11 (1) (2009) 34–40.
- [37] M. Ubartas, J. Rimkeviciene, V. Ostasevicius, V. Jurenas, Experimental investigation of ultrasonically assisted milling, *Proceedings of the 14th International Conference Mechanika*, Kaunas, April 2009, pp. 411–414.
- [38] K.J. Bathe, E.L. Wilson, in: *Numerical Methods in Finite Element Analysis*, Prentice-Hall, Englewood Cliffs, NJ, 1976.
- [39] V. Jurenas, A. Bubulis, I. Skiedraite, V. Ostasevicius, J. Grazeviciute, Tool jaw with ultrasonic transducer, Patent of Republic of Lithuania B23C 9/00 No. LT 5586 B.
- [40] Standards Committee of the IEEE Ultrasonics, Ferroelectrics and Frequency Control Society, IEEE Standard on Piezoelectricity, American National Standards Institute, New York, 1988.
- [41] V. Ostasevicius, V. Jurenas, J. Grazeviciute, A. Bubulis, I. Skiedraite, Quality control system of processed surface, Patent of Republic of Lithuania B23B 1/00 No. LT 5534 B.